Journal of Advanced Marine Engineering and Technology, Vol. 50, No. 2, pp. 100~109, 2026
J. Advanced Marine Engineering and Technology (JAMET)
https://doi.org/10.5916/jamet.2026.50.2.100

ISSN 2234-7925 (Print)
ISSN 2765-4796 (Online)
Original Paper

Tri-generation cascade of s-CO_2 Brayton-Rankine-absorption chiller cycles for WHRS in zero-emission marine systems

Thi Thu Ha TO[1] · Changmin LEE[2] · Jinwon JUNG[3] · Borim RYU[4] · Hokeun KANG†

(Received November 28, 2025 ; Revised February 19, 2026 ; Accepted March 31, 2026)

Abstract: The proposed integrated system consists of a supercritical CO_2 Brayton cycle (s-CO_2), a steam Rankine cycle (SRC) and a LiBr-H_2O absorption chiller (ABS) to utilize exhaust gas from fuel-cell-based marine systems. A thermodynamic model is implemented based on energy and exergy balances for all components. The model has been investigated and simulated in MATLAB and Aspen HYSYS V12.1. The outcomes indicate that the first-tier s-CO_2 Brayton cycle generates 28.6 kW of useful power with a thermal efficiency of 18.9%, while releasing 29.9 kW of recoverable heat to the heat recovery system (HRSG). Next, the SRC recovers 6.35 kW as additional power with an extra thermal efficiency of 21.3%. In addition, the total system generates 34.9 kW of net electric power, and 13.2kW of ABS cooling from 150.4 kW of heat input including cooling, corresponding to 23.2% net electric efficiency and 32.0% overall energy utilization including cooling. The major contributors to the system exergy destruction are the immediate Brayton and bottoming ABS generator. Additionally, the added absorption chiller could make use of the subzero chilling function of LNG or Ammonia storage tanks and the IMO decarbonization framework by the year 2050. Therefore, the proposed waste -to- power design is considered a capable, compact, and scalable approach for next-generation marine systems, principally in fuel-cell integrated designs and exhaust gas utilizing multi-cascade.

Keywords: Waste-to-power, Tri-generation WHRS, Heat recovery system, Cold energy utilization, Decarbonization

1. Introduction

Decarbonization of marine propulsion is becoming an emerging challenge in reaching the International Maritime Organization (IMO) net-zero framework in the next two decades **[1]**. However, traditional diesel-powered vessels, even when partially substituted by liquefied natural gas (LNG), remaining carbon-intensive and thermodynamically constrained impact on ship fleet operations **[2]**. These engines are usually partially utilized the exhaust gas after the conventional engines, notwithstanding low recovery capacity, about 50% **[3]-[4]**. Conventional marine propulsion systems predominantly based on diesel and LNG engines that no longer aligned with IMO GHG reduction and net-zero framework due to tremendous carbon emissions and low waste heat utilization capability as shown in **Figure 1 [5]**. Aligning with existing limitations elimination, zero-carbon renewable fuels commenced a fuel transient fuel conversion efficiency and safety concerns in low-flashpoint storage technologies. Regarding this phenomenon, renewable energies such as ammonia and hydrogen

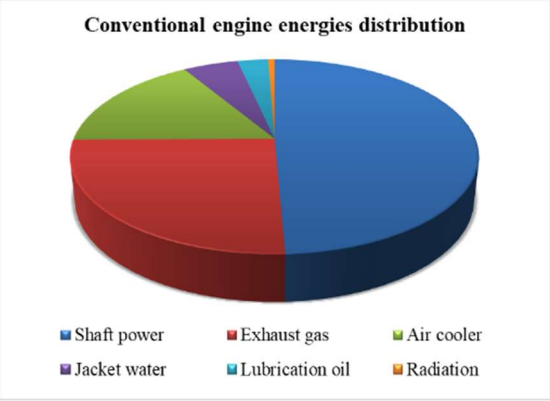

Figure 1: Conventional engines energies distribution **[5]**

† Corresponding Author (ORCID: https://orcid.org/0000-0003-0295-7079): Professor, Department of Marine System Engineering, Korea Maritime & Ocean University, 727, Taejong-ro, Yeongdo-gu, Busan 49112, Korea, E-mail: hkkang@kmou.ac.kr, Tel: 051-410-4862
1 Ph. D. Candidate, Department of Marine System Engineering, Korea Maritime and Ocean University, E-mail: hato20237132@g.kmou.ac.kr
2 Researcher, Maritime Industry Research Institute, Korea Maritime and Ocean University, E-mail: oldbay@kmou.ac.kr
3 Researcher, Carbon Neutrality Technology Research Team, Fuel Gas Technology Center, Alternative Fuel Headquarters, Korea Marine Equipment Research Institute, Busan, South Korea
4 Researcher, Korea Marine Equipment Research Institute, Busan, South Korea

are promising for both thermodynamics properties and environmental requirements on Ozone Depletion Potential (ODP) figure and Global Warming Potential (GWP) measured number **[5]**. However, the worldwide application is limited due to an insufficient regulatory framework on safety operation, risk assessment and systematic bunkering and storage facilities **[6]-[7]**.

State-of-the-art high-temperature electrochemical and closed-cycle technologies, naming fuel-cell gathered systems, nuclear reactors and supercritical CO_2 (s-CO_2) Brayton systems have commenced for efficient, compact marine power generation **[8]-[9]**. Advanced hybrid systems recovering the waste heat from these high-temperature cycles with multi-stage thermal recovery layers have been introduced to stabilize the overall system energy and exergy efficiencies. In addition, Song *et al.* investigated a s-CO_2 Brayton cycle integrated with an organic Rankine cycle that enhances the system thermal energy from 16.4% to 18.1% **[10]**. In another study, an improvement of 2.29% energy and 2.54% exergy efficiencies was seen in the combination of s-CO_2-ARS (Absorption refrigeration system) **[11]**. However, most previous studies focus on individual subsystems such as ideal Brayton and Rankine cycles that speculate constant specific heat or faultless heat exchangers, resulting in differences when extended to real-fluid operation and shipboard integration **[12]-[15]**. Fuel cells and gas turbines are examples of innovative propulsion technologies that require sophisticated thermal-management techniques to enhance efficiency and eliminates toxic emissions. The small size and strong thermal-to-electrical conversion potential of closed-cycle CO_2 Brayton systems make them especially interesting for high-efficiency naval power applications **[16]**. Previous CCHP studies mainly focus on idealized sCO_2-ORC or SOFC-GT systems operating under constant specific heat assumptions **[17]-[18]**. Regarding the current phenomenon, introducing a three-layer cascade of a Brayton cycle, an SRC, and an absorption chilling cycle is necessary. In which, both low-grade absorption cooling and high-temperature heat streams were converted into useful works, in other words, the CO_2-based Brayton-Rankine-ABS configuration successfully addresses the global environmental requirements. The main contribution is the multi-tier validation methodology and the enhancement of thermal energy and electricity generation. At the lowest cycle, the added ABS demonstrates advantageous features for LNG or ammonia fuel onboard storage systems. Thus, the developed configuration commences a viable approach for high temperature outputs such as SOFC-GT, and nuclear-powered engines.

In light of this, the real-fluid CO_2 properties close to the critical area have been used to create a rigorous energy-exergy model of an integrated closed-loop s-CO_2 Brayton-steam Rankine-LiBr-H_2O absorption (ABS) tri-generation system. To guarantee consistency in cycle performance and heat-recovery predictions, the thermodynamic framework is implemented using a UA-NTU-based heat-exchange representation and tested against process-level simulations in Aspen HYSYS. For a typical maritime waste-heat recovery application, the exergy distribution between the Brayton, Rankine, and ABS tiers as well as the overall and subsystem energy and exergy efficiency are assessed. Lastly, a parametric sensitivity analysis is carried out with regard to Brayton pressure ratio, recuperator NTU, and minimum temperature difference in order to find workable design windows that optimize system-level performance while still being consistent with shipboard space, weight, and operation constraints.

2. System Modeling Methodology

2.1 Integrated Hybrid Cycle Configuration Description

Figure 2 provides the structural illustration for the hierarchy energy-management strategy adopted in this study. The overall system integrates an s-CO_2 Brayton topping cycle, a steam Rankine bottoming cycle (SRC) and an absorption refrigeration system (ABS) arranged in a three-tier temperature cascade. The figure clarifies the energy flow direction and the hierarchical heat-grade matching from the high-temperature exhaust gas stream to the medium and low-temperature streams. To ensure transparent and reproducible thermodynamic molding, **Figure 3** demonstrates the integrated cascade configuration, specifying the interconnections and thermodynamic interfaces for heat-transfer duties, pressure losses as well as energy balances.

The heat and mass balance principles serve as the foundation for the invention, which is logically energy hierarchy management:

- Tier I: Working in the highest-grade heat (800-1000K), from the SOFC-GT or nuclear reactors exhaust drives the Brayton loop. The working fluid s-CO_2 streams continuously within a closed circle, maximizing energy and exergy efficiency as well as eliminating the thermal energy extraction to the surrounding environment.
- Tier II: Operating in the medium-grade heat from 500K to 600K, the steam Rankine turbine converts the upper exhaust gas after Brayton turbine to govern the middle cycle.
- Tier III: Working under the lowest-grade heat from 370K to 400K, in which the middle cycle exhaust gas has been transferred to the ABS, supplying cold energy for onboard demands and chilling storage purposes.

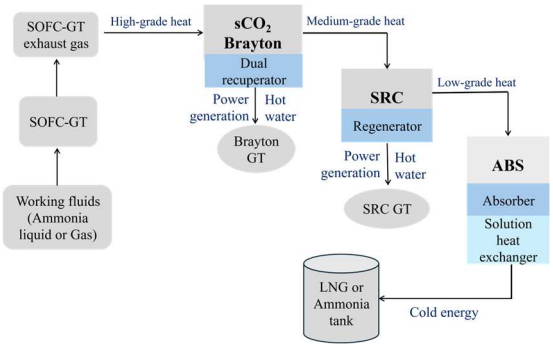

Figure 2: The s-CO_2 Brayton-SRC-ABS energy hierarchy

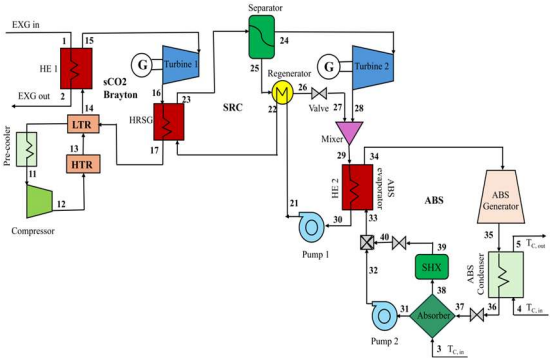

Figure 3: The integrated waste-heat cascade and ABS cooling system

The heating and cooling integration commences a new era of thermodynamic principle applications in marine engineering due to a considerable improvement of overall energy and exergy efficiency.

2.2 Thermodynamic Modeling

The proposed design has been divided into three main tiers with the combination of Braton cycle recovering the waste heat from the 700ºC thermal waste source, while the second layer presenting the possibility to utilize the waste heat from 150-250ºC and the bottoming cycle recovering the low-grade heat from 80-100ºC. By integrating three different thermal cycles together, the waste heat source can be efficiently utilized. The integrated system was modelled as a unified thermodynamic framework combining a closed CO_2 Brayton cycle, dual recuperators, a HRSG-Rankine loop, and an absorption chiller. Each subsystem was defined using energy balance and $NTU - \varepsilon$ correlations. Parametric tables allowed the adjustment of variables such as T_3, PR, NTU_{HTR}, and HRSG pinch. In this study, the system is formulated as an analytical thermodynamic model based on coupled mass/energy and exergy balances, together with UA-NTU heat-exchanger relations. The resulting state-point equations are solved in MATLAB using an iterative convergence routine, which also enables automated parametric sweeps of key design and operating variables. The modeling framework develops analytical

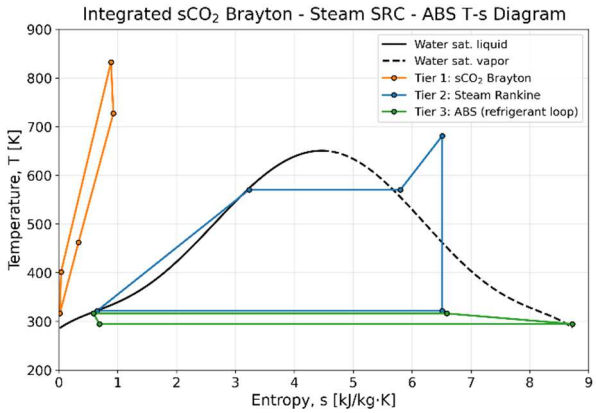

Figure 4: Three-tier sCO_2-RC-ABS cascade T-s diagram

energy and exergy balancing equations with real-fluid thermodynamics evaluation and process-level validation using Aspen HYSYS V12.1 software. The mathematical calculations support the consistent modeling of s-CO_2 Brayton, SRC, and LiBr-H_2O absorption cooling within thermodynamic simulation conditions.

To build up the computational consistency, steady-state operational and one-dimensional flow conditions are assumed for the subsystems. First, the pressure drop ratio has been calculated at 3% within pipeline system and heat exchangers while the kinetic and potential energy differences are ignored. The unified analysis of power and cooling generation is governing and enabling by an energy and exergy balancing as well as the UA-NTU heat-transfer modeling. The working fluid CO_2 thermodynamic characteristics are calculated under Helmholtz energy equation close to the critical point at 304.13K and 7.38 MPa. Component efficiencies are based on typical marine-scale turbomachinery with turbine energy efficiency is 0.9, compressor efficiency is 0.85 and compact heat exchanger efficiency is 0.9. For any component i such as turbine, compressor, heat exchanger, or pump, the steady-state energy balance is written under the first law of thermodynamics:

$$\dot{Q}_i - \dot{W}_i = \sum_{out} \dot{m} h_{out} - \sum_{in} \dot{m} h_{in} \quad (1)$$

Where $\dot{W}_i$ is the shaft work (kW), $\dot{m}$ is the mass flow rate (kg/h), h is the specific enthalpy (kJ.kg^{-1}). The compressor and turbine are investigated under the isentropic efficiencies:

$$\eta_T = \frac{h_{in} - h_{out}}{h_{in} - h_{out,s}}; \quad \eta_{Comp} = \frac{h_{out,s} - h_{in}}{h_{out} - h_{in}} \quad (2)$$

In which, the subscript s denotes the isentropic state. The compressor and turbine work outputs are calculated by **Equation (3)**:

$$\dot{W}_T = \dot{m}(h_{in} - h_{out}); \qquad \dot{W}_C = \dot{m}(h_{out} - h_{in}) \quad (3)$$

Regarding the CO_2 stream, the amount of total heat transferred to the HRSG is measured:

$$Q_{HRSG} = \dot{m}_{CO_2}(h_{T,out} - h_{T,in}) \quad (4)$$

While the steam-side balance is:

$$Q_{HRSG} = \dot{m}_{steam}(h_{evap,out} - h_{evap,in}) \quad (5)$$

High-temperature exhaust gases from the SOFC-GT subsystem are supplied to the s-CO_2 Brayton cycle, which then sends recovered heat to the steam Rankine loop via the HRSG. The Rankine condenser rejects residual thermal energy to power the ABS chiller, creating a chilled stream at 260K suitable for storing LNG or ammonia.

To minimize energy losses, each subsystem is thermally coupled to provide a closed-loop tri-generation configuration. The dual recuperators and the HRSG have been governed by the Thermodynamics law and modeled through the UA-NTU calculation to investigate the fluctuations of supercritical CO_2 working fluid. This method couples the overall heat-transfer coefficient (UA) and effectiveness (ε) to the logarithmic mean and variable heat capacities:

$$\varepsilon = \frac{Q}{C_{min}(T_{h,in} - T_{c,in})} \quad (6)$$

$$NTU = \frac{UA}{C_{min}}; \qquad \varepsilon = \frac{1 - e^{-NTU(1-C_r)}}{1 - C_r e^{-N \quad (1-C_r)}} \quad (7)$$

$$Q = UA * \Delta T_{lm} = \varepsilon C_{min}(T_{h,in} - T_{c,in}) \quad (8)$$

Where UA is the overall heat-transfer conductance (W.K-1); C_{min} and C_{max} are the minimum and maximum heat capacity rates and $C_r = \frac{C_{min}}{C_{max}}$. By comparing analytical UA-NTU predictions with ASPEN HYSYS calculated heat exchanger duties, the method offers a rigorous validation basis. The LiBr-H_2O absorption chiller uses Rankine condenser heat Q_{gen} to transfer the cold energy for LNG tank or ammonia storage with the fixed evaporator temperature at T_{evap}= 260K, the coefficient of performance is:

$$COP_{abs} = \frac{Q_{evap}}{Q_{gen}} \quad (9)$$

This stage enables sub-zero thermal management, serving cryogenic storage of low flashpoint fuels. Building upon the general steady-state formulation above, the present work isolates the Brayton-Rankine-ABS thermodynamic subsystem to evaluate its independent performance without the SOFC primary source. In this configuration, the external heat input to the Brayton heater represents the available high-temperature energy from any upstream prime mover (e.g., SOFC, nuclear reactor, or gas-turbine exhaust), whereas the subsequent Rankine and absorption stages recover the medium- and low-grade heat in cascade. The same first-law and UA-NTU relations introduced in **Equation (1) – Equation (9)** are retained, while the fuel-based chemical-exergy expressions are omitted. Accordingly, the following section develops explicit component-level relations (compressor, turbine, recuperators, HRSG, and ABS) and defines the system energy and exergy efficiencies within a self-contained Brayton-Rankine-ABS framework.

2.3 Integrated Modelling Assumptions

Based on the energy-balance formulation described in the previous section, the integrated configuration couples a closed supercritical CO_2 Brayton cycle (topping) with a single-pressure steam Rankine bottoming cycle and a LiBr-H_2O absorption refrigeration system(ABS). The methodology follows Mubashir *et al.* **[19]**, in which energy and exergy balances are applied to each subsystem linked through cascading heat recovery. Main simulations are assumed as below:

- Steady-state, potential and kinetic energies neglected.
- Real-fluid thermodynamic properties of CO_2 are used in all cycle calculations, and no constant c_p ideal gas approximation is applied in the final performance evaluation
- Pressure drop ratio is 3% **[20][21]**
- Counter-flow heat exchangers solved via $NTU - \varepsilon$
- Fluid equilibrium at each component boundary.

To ensure realistic and safe operation, several design limits were imposed prior to the thermodynamic evaluation. The minimum temperature difference in the recuperators prevents numerical divergence in the $NTU - \varepsilon$ model and ensures feasible counter-flow heat transfer. The HRSG pinch point was fixed at 8K to limit excessive surface area and pressure drop, while the Brayton turbine inlet temperature was restricted to be smaller than 900K due to material constraints. These constraints were applied in all subsequent simulations and parametric analyses.

Compression: state 1- 2

$$T_{2s} = T_1 \left(\frac{P_2}{P_1}\right)^{\frac{k_1-1}{k_1}}; h_{2s} = h_1 + c_{p,c}(T_{2s} - T_1); h_2 = h_1 + \frac{h_{2s} - h_1}{\eta_{comp}} \quad (10)$$

$$w_{comp} = c_{p,c}(T_2 - T_1) \quad (11)$$

Expansion: state 3- 4

$$T_{4s} = T_3\left(\frac{P_4}{P_3}\right)^{\frac{k_3-1}{k_3}};\ h_{4s} = h_3 - c_{p,h}(T_3 - T_{4s});\ h_4 = h_3 - \eta_T(h_3 - h_{4s}) \quad (12)$$

$$w_{Tur} = c_{p,h}(T_3 - T_4) \quad (13)$$

Dual recuperators (LTR & HTR)

$$\varepsilon_i = \frac{1-\exp\left[-NTU_i(1+C_r)\right]}{1+C_r};\ NTU_i = \frac{UA_i}{C_{min}} \quad (14)$$

$$Q_i = \varepsilon_i C_{min}(T_{h,in} - T_{c,in}) \quad (15)$$

$$T_{2r} = T_{2r,LTR} + \frac{Q_{HTR}}{\dot{m}_B c_{p,c}};\ T_{4r} = T_{4r,LTR} + \frac{Q_{HTR}}{\dot{m}_B c_{p,h}} \quad (16)$$

$$\dot{Q}_{in,B} = \dot{m}_B c_{p,h}(T_3 - T_{2r});\ \dot{W}_B = \dot{m}_B(w_{Tur} - w_{comp}) \quad (17)$$

$$\eta_B = \frac{\dot{W}_B}{\dot{Q}_{in,B}} \quad (18)$$

HRSG and Rankine Cycle

Gas-side heat balance

$$T_{g,out} \geq \max\left(T_{sat,bo} + P_{inch}, T_{4r}\right);\ \dot{Q}_{HRSG} = \dot{m}_B c_{p,h}(T_3 - T_{g,out}) \quad (19)$$

Steam-side enthalpy relations

$$T_{sat,bo} = 373.15\left(\frac{P_{bo}}{101.325}\right)^{0.25};\ T_{sat,con} = 373.15\left(\frac{P_{con}}{101.325}\right)^{0.25} \quad (20)$$

$$h_{1w} = 4.18\left(T_{sat,con} - 273.15\right);\ h_{3w} = 2500 + 1.9(T_{sh} - 373.15) \quad (21)$$

$$h_{4w} = h_{3w} - \eta_{Ts}(h_{3w} - h_{g,con});\ w_{p,spec} = v_{l,w}(P_{bo} - P_{con}) * 10^{-3} \quad (22)$$

$$\dot{m}_s = \frac{\dot{Q}_{HRSG}}{h_{3w}-h_{2w}};\ \dot{W}_R = \dot{m}_s[(h_{3w} - h_{4w}) - w_{p,spec}];\ \eta_R = \frac{\dot{W}_R}{\dot{Q}_{HRSG}} \quad (23)$$

$$\dot{Q}_{con} = \dot{m}_s(h_{4w} - h_{1w}) \quad (24)$$

Absorption chiller system (ABS)

$$\dot{Q}_{gen} = f_{abs}\dot{Q}_{con};\ \dot{Q}_{cool} = COP_{abs}\dot{Q}_{gen} \quad (25)$$

$$COP_{abs} = \frac{\dot{Q}_{cool}}{\dot{Q}_{gen}};\ \dot{Q}_{reject} = (1 - f_{abs})\dot{Q}_{con} \quad (26)$$

Energy and exergy efficiencies

$$\eta_{elec} = \frac{\dot{W}_B + \dot{W}_R}{\dot{Q}_{in,B}};\ \eta_{en} = \frac{\dot{W}_B + \dot{W}_R + \dot{Q}_{cool}}{\dot{Q}_{in,B}} \quad (27)$$

$$\eta_{ex} = \frac{\dot{W}_B + \dot{W}_R + \dot{E}_{cool}}{(1-\frac{T_0}{T_S})\dot{Q}_{in,B}} \quad (28)$$

To determine the best design zones for maritime operation, sensitivity analysis on pressure ratio, turbine inlet temperature, and recuperator NTU are carried out. A paramount contribution is carrying out a hybrid multi-platform validation procedure that integrates analytical modeling and process-level simulation in a single thermodynamic environment. The remarkable contribution is governing by the energy and exergy conservation principles aligning with the process simulated in Aspen HYSYS simulator, thus supporting the validation of the multi-tiered design. Additionally, the introduced configuration examines the deployment of Brayton-Rankine-ABS integration, resulting in a modeling technique that is both thermodynamically conservation and operationally capable opportunity.

Off-design modeling assumptions

Exhaust gas mass flow scaling at full load with L is engine load ($L \in \{50,\ 75, 100\}$ and $\dot{m}_{100}$ is the exhaust gas mass flow at 100% load.

$$\dot{m}_{EXG}(\mathrm{L}) = \dot{m}_{100}\mathrm{L} \quad (29)$$

Exhaust gas temperature derating is defined as in **Equation (30)**.

$$\mathrm{T}_{EXG}(\mathrm{L}) = \mathrm{T}_{EXG,100} - k_r(1 - L) \quad (30)$$

where k_r= 100K, yielding $\mathrm{T}_{EXG,75}$= 948K, and $\mathrm{T}_{EXG,50}$= 923K

To present hydraulic losses, pressure losses were simulated under a segment-level lumped allowance approach. The pressure drop is prescribed as a fixed fraction of the local inlet pressure:

$$\Delta P_{seg} = f_{PD}P_{in,seg} \quad (31)$$

The outlet pressure is defined

$$P_{out,seg} = P_{in,seg} - \Delta P_{seg} = (1 - f_{PD})P_{in,seg} \quad (32)$$

A parametric sweep was conducted over $f_{PD} \in \{0.01, 0.03, 0.05\}$ to quantify the impact of plausible hydraulic-loss uncertainty on the key performance indicators.

3. Results and Discussion

3.1 Integrated System Thermodynamics Performance Analysis

The proposed Brayton-steam Rankine-ABS configuration indicates a considerable thermodynamic enhancement over the standalone Brayton or SOFC-GT system. This demonstrates a substantial improvement in thermodynamic performance compared to the conventional marine combined cycles as illustrated in **Table 1**.

Table 1: Subsystem energy and exergy analysis

Subsystem	Power (kW)	External heat input (kW)	Energy performance (%/-)	Exergy performance (%)
s-CO_2 Brayton	28.58	150.4	18.99	29.2
Rankine	6.35	-	21.3	33.3
ABS	13.19 (cooling)	-	COP = 0.7	-
System total	34.93	150.4	32.0	49.2

As the system-level energy efficiency reported, about 32.0% is evaluated according to **Equation (27)** and therefore includes both net electric power and the equivalent primary-energy saving associated with the 13.19 kW of cooling. The total system power output accounted for 34.93 kW, which is sufficiently supplied for onboard demanding energies and served as the extra electric as well as thermal supplying source for heating, accommodation hot water providing, and lubricant oil heating. Overall energy and exergy efficiencies reach 32.0% and 49.2%, representing a 13% improvement over the conventional Brayton baseline from 19% to 32%. The results have validated with the previous study **[22]**.

The topping s-CO_2 Brayton subsystem generates a net power output of 28.58 kW from a total heat input of 150.4 kW, illustrating an energy efficiency of 18.99% and an exergy efficiency $\eta_{ex,B}$= 29.2%. The dual-recuperator Brayton cycle effectively leads to the turbine exhaust temperature growth for efficient heat recovery in the immediate layer, while the ABS chiller utilizes the upper exhaust gas then converts to useful cooling as the thermodynamic characteristics. The s-CO_2 Brayton cycle energy efficiency is significantly affected by the imposed turbine temperature inlet limit (TIT less than 973K) and the finite temperature approaches in the dual recuperators. However, the first cycle recovers an extremely high temperature from the given exhaust gas flow from turbine or recuperator outlet. This heat source is thermodynamically well-matched with the downstream Rankine cycle and thus acts as the principal exergy carrier within the tri-generation design. The exhaust gas exiting the turbine (T4r = 707K) is utilized as the prime heat supplying source for the HRSG in the bottoming Rankine cycle.

The intermediate Rankine cycle operates as a relatively simple single pressure bottoming component. In which, steam vapor is generated thanks to the HRSG generator (HRSG) at a boiler pressure of 2 MPa and condenser pressure of 10 kPa, with a steam turbine efficiency of 0.75. The HRSG extracts 29.91 kW of recovered heat from the Brayton exhaust. The LiBr-H2O absorption chiller recovers 80% of the Rankine condenser heat (fabs= 0.8), in which ABS can efficiently deploy the lowest grade heat that rejecting from the Rankine condenser. With a coefficient of performance (COPabs= 0.7), the system delivers 13.19 kW of cooling ability at the boiling temperature of 260K and a generator source temperature of approximately 580K. Although the exergy efficiency of this low-temperature subsystem is lower than that of the power cycles, the cooling capacity is sufficient to support sub-ambient services such as fuel pre-cooling, boil-off reduction in LNG or ammonia tanks, or refrigerated cargo, thereby converting residual thermal losses into operationally valuable refrigeration. By efficiently converting low-temperature waste heat into usable refrigeration, this step improves system utilization overall. The steam generated passing by the SRC turbine, in the next stage producing 6.35 kW of net power. The Rankine subsystem exhibits a cycle efficiency of approximately 21.3% and exergy efficiency of 33.3%, contributing about 18% of the total electrical output.

The exergy distribution among subsystems clarifies their respective roles in exergy recovery. Despite the Brayton cycle being the primary source of mechanical power, the bottoming units account for a substantial fraction of the useful exergy. As shown in **Figure 5**, the Rankine cycle exhibits the highest exergy efficiency (33.3%), whereas the Brayton and ABS subsystems reach 29.2% and 16.4%, respectively. The Rankine, Brayton, and ABS subsystems contribute roughly 42%, 37%, and 21% of the total recovered exergy. These numbers show that the cascaded Rankine and ABS stages together recover a significant portion of the available exergy that would otherwise be destroyed or rejected, even though the topmost s-CO_2 Brayton cycle serves as the primary driving power. This distribution indicates that, although the topping cycle provides the main driving potential, the cascaded bottoming stages collectively recover the majority of exergy that would otherwise be destroyed or rejected, emphasizing that system-level design is more effective than isolated optimization of the topping cycle alone.

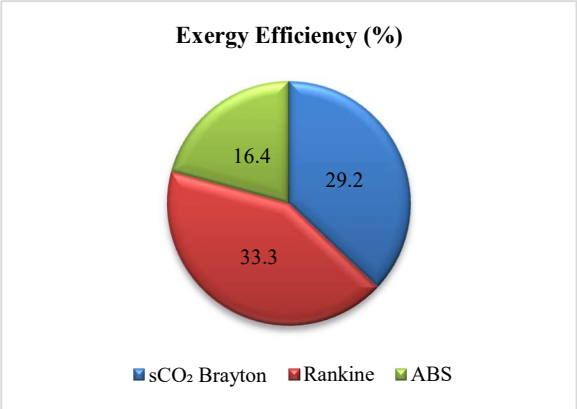

Figure 5: Three-tiered Brayton-SRC-ABS exergy efficiency

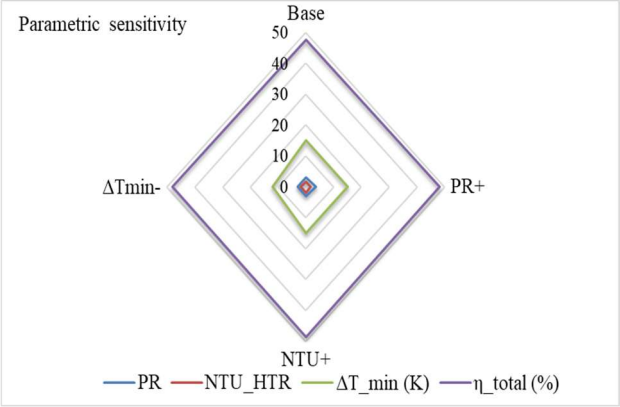

Figure 6: Parametric sensitivity analysis

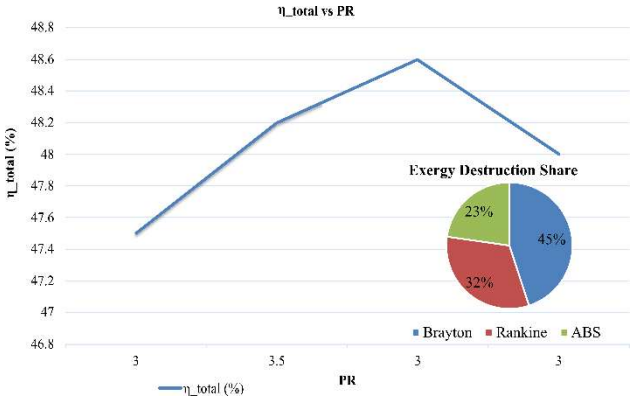

Figure 7: Trade-off between design PR and irreversibility

3.2 Design-Parameter Sensitivity and Optimization

The influence of key design and operating parameters on the system energy efficiency of the tri-generation system is examined through a parametric sensitivity analysis stage. The analysis considered several key parameters such as Brayton pressure ratio, the minimum temperature difference in the recuperators and the overall heat transfer conductance expressed via the number of transfer units (NTU) for the dual recuperators. Over the investigated range, the total energy efficiency $\eta_{en,tot}$ increases almost linearly with PR, reflecting higher specific work and a higher mean temperature of heat addition in the Brayton cycle as PR rises. The figures for the minimum temperature difference (ΔT_{min}), the overall heat-transfer conductance of the recuperators, and pressure ratio have been investigated under different layers with the aim of examining the maximized margins of system overall energy efficiency as illustrated in **Figure 6**.

However, as illustrated in **Figure 7**, this gain is accompanied by a rise in irreversibility associated with increased compression work and larger temperature differences in the recuperators at off-design points. Consequently, there exists a practical PR window in which the total system energy value is significantly enhanced while the marginal penalty in exergy destruction and mechanical complexity remains acceptable for marine applications. Similarly, an increase in recuperator NTU (for both LTR and HTR) improves the internal temperature matching of the s-CO_2 streams, leading to a higher preheat level at the Brayton heater inlet and a lower exhaust temperature entering the HRSG. This simultaneously increases Brayton-cycle efficiency and the quality of heat supplied to the Rankine system. The results indicate that $\eta_{en,tot}$ is sensitive to NTU in the low-to-moderate range but exhibits diminishing returns as NTU becomes large, where the effectiveness approaches its asymptotic limit while heat-exchanged area, cost, and pressure drop continue to increase.

As demonstrated in **Figure 7**, at PR= 3.5, the overall energy accounts for 32% total energy. Beyond this point, the additional compressor work offsets turbine expansion benefits. Exergy analysis indicates 45%, 32%, and 23% destruction in the Brayton, Rankine, and ABS subsystems, respectively. This confirms that recuperator enhancement remains the primary pathway for efficiency improvement and quality of the heat supplied to the Rankine system. It is indicated that total energy is sensitive to NTU in the low-to-moderate heat range, but as NTU increases, its effectiveness approaches its asymptotic limit, whereas the heat exchanger size and pressure drop continue to rise. High irreversibility and poor utilization of low-grade heat are main elements limiting the waste heat recovery potential of conventional diesel and LNG-fueled vessels.

When interpreted in a marine context, these findings have direct practical implications. The three-tier architecture aligns naturally with the temperature hierarchy of typical shipboard energy streams: high-temperature exhaust from a prime mover (SOFC, gas turbine, or nuclear reactor) is processed in the s-CO_2 Brayton cycle; medium-temperature heat is recovered in the steam Rankine cycle; and low-grade heat is converted into useful cooling in the ABS chiller. The compactness of s-CO_2 turbomachinery and printed-circuit-type heat exchangers facilitates integration in space- and weight-constrained engine rooms, whereas the Rankine and ABS modules can be implemented as modular skids interfacing with existing exhaust-gas and cooling-water circuits. The 13.19 kW of cooling produced by the ABS at 260K can be flexibly allocated to accommodation HVAC, refrigerated cargo, or cryogenic fuel services, thereby reducing the operating hours of conventional electrically driven chillers and auxiliary compressors.

3.3 Robustness under Operating-Condition Variations

Marine waste-heat recovery systems are predominantly clustered around part-load conditions due to engine load fluctuations and

Table 2: Engine-load sensitivity analysis

Load (%)	$\dot{m}_{EXG}$ (kg/h)	T_{EXG} (K)	Brayton Power (kW)	Rankine Power (kW)	ABS Cooling (kW)	System Power (kW)
50	6000	923	14.29	3.18	6.6	17.47
75	9000	948	21.44	4.76	9.89	26.2
100	12000	973	28.58	6.35	13.19	34.93

Table 3: Net power vs pressure-drop sensitivity analysis

DP (%)	ΔP_{shell} (kPa)	ΔP_{tube} (kPa)	$W_{net,total}$ (kW)	η_{en} Include cooling (%)	ΔW_{net} vs DP 3% (%)
1	60	20	36.33	32.9	4.01
3	180	60	34.93	32	0
5	300	100	33.57	31.1	-3.89

installation-dependent hydraulic losses in heat exchangers and piping. To capture off-design operation, the exhaust gas boundary conditions are parameterized as a function of engine load. The engine load is set at 50%, 75%, and 100% and for each load case, the resulting performance trends are analyzed to identify whether power and cooling outputs remain within an acceptable range for practical deployment.

In addition, the overall pressure-drop ratio necessitates due to uncertainty in hydraulic losses which can further shift the operating point. Thus, the changes in net power output and absorption cooling capacity, referenced to the baseline, define the off-design performance envelope and support the selection of resilient setpoints. **Table 2** shows near-linear scaling with engine load as $\dot{m}_{EXG}$ doubles from 6000 to 12000 kg/h, T_{EXG} increases slightly from 923K to 973K, the $W_{net,total}$ rises from 17.47 to 34.93 kW. The power split remains essentially constant, indicating 82% Brayton, 18% Rankine while ABS cooling increases from 6.6 to 13.19 kW.

As demonstrated in **Table 3**, the pressure-drop sweep (1-5%) indicates that cycle performance is weakly sensitive to the assumed uniform hydraulic-loss margin. Increasing the loss factor increases the imposed drops (ΔP_{Shell} in the range of 60-300 kPa; ΔP_{tube} in the range of 20-100 kPa) and lowers net output from 36.33 kW (1%) to 33.57 kW (5%). Importantly, the 3% baseline lies near the center of this band: relative to 3% (34.93 kW), net power changes by only +4.01% (pressure drop 1%) and -3.89% (pressure drop 5%), and efficiency overall decreases modestly from 32.9% to 32%. This bounded response shows that the key conclusions are not artifacts of the pressure-drop assumption; rather, ΔP mainly shifts absolute KPIs without altering trends. Therefore, adopting ΔP = 3% is a reasonable and conservative screening-level allowance representing aggregated exchanger/piping/minor losses under concept-design uncertainty.

4. Conclusions

The proposed tri-generation configuration provides additional operational flexibility by allowing the s-CO_2 Brayton and steam Rankine cycles to be prioritized for maximizing net electrical output at sea, while shifting control toward the absorption refrigeration system (ABS) to secure critical cooling under low-load or port conditions. This operating flexibility can reduce reliance on auxiliary power generation and supports lower specific CO_2 emissions per transport work, aligning with tightening IMO energy-efficiency and greenhouse-gas requirements. Apart from these global remarking regulatory changes and renewable energies transient, waste heat recovery innovations have considered leading and dominant priority in the shipping industry as an alignment with IMO net-zero framework by 2050. The key findings are summarized as below:

① Development of a real-fluid heat exchange model capturing CO_2 property variations near the critical region, capturing accurately and providing precise UA-NTU based investigation recuperator performance.

② The implementation of a three-tier thermodynamic coupling mechanism that cascades exergy from different heat layers, maximizing total thermal efficiency of the chosen working fluids. By carrying a systematic review, it is indicated that no previous study has investigated a closed-loop s-CO_2 Brayton-WHRS-ABS system, existing studies focusing on SOFC-Brayton or SOFC-Rankine combination separately. This is the first fully integrated supercritical CO_2 Brayton-SRC-ABS framework, aiming at waste heat recovery maximization and generating extra electricity from the rich potential thermal source.

③ The dual recuperator optimization technique that identifies optimal design points, with 32% energy and 49.2% exergy are competitive with reported marine waste heat cascades in the literature.

④ Thanks to the unceasing streams of low-flashpoint fuels and an integrated cryogenic fuel system, offering potential solution for future coupling with cold-energy recovery from LNG and ammonia tanks. As a result, the power-heat-cooling design could serve as a new benchmark in fully optimized onboard waste heat applications.

The research objectives are investigating, developing and validating the first demonstrably combination of a s-CO_2 Brayton-WHRS-

ABS system, that capable of delivering simultaneous power, heating, and cooling in a compact and fully emission-free configuration.

Acknowledgement

This research was supported by Korea Evaluation Institute of Industrial Technology (KEIT) grant funded by the Ministry of Trade, Industry and Energy (MOTIE) (RS-2023-00285272, RS 2024-00434535 and RS-2024-00458498). This work was supported by Korea Institute for Advancement of Technology (KIAT) grant funded by the Korean Government (MOTIE) (RS-2025-02215617, HRD Program for Industrial Innovation).

Author Contributions

Conceptualization, T.T.H To, H.K Kang; Methodology, T.T.H To; Software, T.T.H To; Formal Analysis, T.T.H To; Investigation, T.T.H To; Resources, T.T.H To, C. Lee; Data Curation T.T.H To, C. Lee; Writing-Original Draft Preparation, T.T.H To; Writing-Review & Editing, T.T.H To, H.K Kang; Visualization, T.T.H To, C. Lee; Supervision, H.K Kang; Project Administration, H.K Kang; Funding Acquisition, H.K Kang.

References

[1] IMO (2023, July 7), Marine Environment, Retrieved from 2023 IMO Strategy on Reduction of GHG Emissions from Ships: https://www.imo.org/en/ourwork/environment/pages/2023-imo-strategy-on-reduction-of-ghg-emissions-from-ships.aspx

[2] S. Ha and B. Jeong, H. Jang, C. Park, and B. Ku (2023), "A framework for determining the life cycle GHG emissions of fossil marine fuels in countries reliant on imported energy through maritime transportation: A case study of South Korea," Science of the total environment, vol. 897, 165366, 2023.

[3] S. Zhu, Z. Ma, K. Zhang, and K. Deng, "Energy and exergy analysis of a novel steam injected turbo-compounding system applied on the marine two-stroke diesel engine," Energy Conversion and Management, vol. 221, 113207, 2020.

[4] L. A. Díaz-Secades, R. González, and N. Rivera, "Waste heat recovery from marine engines and their limiting factors: Bibliometric analysis and further systematic review," Cleaner Energy Systems, vol. 6, p. 100083, 2023.

[5] W. Zhang, J. Wang, G. Qin, S. Kuntal, F. Gong, and R. Yan, "Review of the state-of-the-art of alternative marine fuels: A viable approach to zero-carbon shipping," Cleaner Logistics and Supply Chain, vol. 16, p. 100232, 2025.

[6] Q. Wang, H. Zhang, J. Huang, and P. Zhang, "The use of alternative fuels for maritime decarbonization: Special marine environmental risks and solutions from an international law perspective," Frontiers in Marine Science, vol. 9, p. 1082453, 2023.

[7] Y. Li, Y. Zhou, J. Shi, and K. F. Yuen, "Alternative marine fuel adoption: Probabilistic risk assessment and mitigation for informed policymaking," Transportation Research Part D: Transport and Environment, vol. 150, p. 105080, 2026.

[8] B. V Veldhuizen, L. V Biert, P. V. Aravind, and K. Visser, "Solid oxide fuel cells for marine applications.," International Journal of Energy Research, vol. 2023, no. 1, p. 5163448, 2023.

[9] P. Wu, Y. Ma, C. Gao, W. Liu, J. Shan, Y. Huang, J. Wang, D. Zhang and X. Ran, "A review of research and development of supercritical carbon dioxide Brayton cycle technology in nuclear engineering applications," Nuclear Engineering and Design, vol. 368, p. 110767, 2020.

[10] J. Song, X. S Li, X. D Ren, and C.W Gu, "Performance analysis and parametric optimization of supercritical carbon dioxide (S-CO_2) cycle with bottoming Organic Rankine Cycle (ORC)," Energy, vol. 143, pp. 406-416, 2018.

[11] C. Wu, X. Xu, Q. Li, J. Li, S. Wang, and C. Liu, "Proposal and assessment of a combined cooling and power system based on the regenerative supercritical carbon dioxide Brayton cycle integrated with an absorption refrigeration cycle for engine waste heat recovery," Energy Conversion and Management, vol. 207, p. 112527, 2020.

[12] A. Yu, W. Su, X. Lin, and N. Zhou, "Recent trends of supercritical CO_2 Brayton cycle: Bibliometric analysis and research review," Nuclear Engineering and Technology, vol. 53, no. 3, pp. 699-714, 2021.

[13] E. Wang, N. Peng, and M. Zhang, "System design and application of supercritical and trans-critical CO_2 power cycles: A review," Frontiers in Energy Research, vol. 9, p. 723875, 2021.

[14] M. E. Mondejar, J. G. Andreasen, L. Pierobon, U. Larsen, M. Thern, and F. Haglind, "A review of the use of organic Rankine cycle power systems for maritime applications," Renewable and Sustainable Energy Reviews, vol. 91, pp. 126-151, 2018.

[15] F. Reale and P. Massoli, “WHR systems based on sCO_2 gas turbines for marine applications: The effect of route environmental conditions on performance,” Energy Conversion and Management: X, X26, p. 100915, 2025.

[16] J. Feng, J. Wang, Z. Chen, Y. Li, Z. Luo, and B. Bai, “Performance advantages of trans-critical CO_2 cycle in the marine environment,” Energy, vol. 305, p. 132251, 2024.

[17] R. Zeng, J. Gan, B. Guo, X. Zhang, H. Li, W. Yin, and G. Zhang, “Thermodynamic performance analysis of solid oxide fuel cell - combined cooling, heating and power system with integrated supercritical CO_2 power cycle-organic Rankine cycle and absorption refrigeration cycle,” Energy, vol. 283, p. 129133, 2023.

[18] S. Yang, Z. Jin, F. Ji, C. Deng, and Z. Liu, “Proposal and analysis of a combined cooling, heating, and power system with humidity control based on solid oxide fuel cell,” Energy, vol. 284, p. 129233, 2023.

[19] W. Mubashir, M. Adnan, M. Zaman, M. Imran, S. R. Naqvi, and A. Mehmood, “Thermo-economic evaluation of supercritical CO_2 Brayton cycle integrated with absorption refrigeration system and organic Rankine cycle for waste heat recovery,” Thermal Science and Engineering Progress, vol. 44, p. 102073, 2023.

[20] F. Correa, R. Barraza, Y. C. S. Too, R.V. Padilla, and J. M. Cardemil, “Optimized operation of recompression sCO_2 Brayton cycle based on adjustable recompression fraction under variable conditions,” Energy, vol. 227, p. 120334, 2021.

[21] M. S. Yousef and D. Santana, “Energy and exergy analyses of a recompression supercritical CO_2 cycle combined with a double-effect parallel absorption refrigeration cycle,” Energy Reports, vol. 9, Supplement 12, pp. 195-201, 2023.

[22] Y. Que, Z. Hu, S. Ren, and Z. Jiang, “Thermodynamic analysis of a combined recompression supercritical carbon dioxide Brayton cycle with an organic flash cycle for hybrid solar-geothermal energies power generation,” Frontiers in Energy Research, vol. 10, 924134, 2022.